



OPEN

Experimental solubility and modeling of Crizotinib (anti-cancer medication) in supercritical carbon dioxide

Gholamhossein Sodeifian^{1,2,3✉}, Chandrasekhar Garlapati⁴ & Armin Roshanghias^{1,2,3}

Measurement of saturation solubility of drugs in a supercritical fluid is an important parameter for the implementation of supercritical technology in pharmaceutical industry. CO₂ is the most sorted substance as a supercritical fluid since it has attractive properties like easily achievable critical temperature, moderate pressure. Cancer is increasingly affecting the mankind, a proper dosage while treating would help in minimizing the drug usage. The bioavailability of the drug is mainly influenced by the drug particle size. An appropriate technology is always useful in making suitable drug particles; thus, supercritical fluid technology (SFT) is considered as promising technique for the production of micro and nanoparticles. Since, particle production process through SFT needs solubility information, appropriate solubility information is necessary. In the present work, Crizotinib (anti-cancer drug) solubility in supercritical carbon dioxide (scCO₂) is measured and reported, for the first time. The obtained solubilities are at temperatures 308, 318, 328, 338 K and pressures 12, 15, 18, 21, 24 to 27 MPa. The measured solubilities are ranged in terms of mole fraction from $(0.483 \times 10^{-5}$ to 0.791×10^{-5}) at 308 K, $(0.315 \times 10^{-5}$ to 0.958×10^{-5}) at 318 K, $(0.26 \times 10^{-5}$ to 1.057×10^{-5}) at 328 K, $(0.156 \times 10^{-5}$ to 1.219×10^{-5}) at 338 K. The cross over region is observed at 14.5 MPa. To expand the application of the solubility data, few important solubility models and three cubic equations of state (cubic EoS) models along with Kwak and Mansoori mixing rules are investigated. Sublimation and salvation enthalpies of Crizotinib dissolution in scCO₂ are calculated.

List of symbols

A_1, B_1	Adjustable parameters for Eqs. (6), (7)
A_2, B_2	Adjustable parameters for Eq. (8)
A_3, B_3, C_3	Adjustable parameters for Eq. (9)
A_4, B_4, C_4	Adjustable parameters for Eq. (10)
AARD%	Percent of average absolute relative deviation
AIC	Akaike information criterion
AIC_c	Corrected AIC
C_s	Concentration of drug inside collection vial in g/L
E1- A14	Apparatus symbols
H_{sol}	Crizotinib solvation enthalpy in kJ/mol
H_{vap}	Crizotinib vaporization enthalpy in kJ/mol
H_{tot}	Total enthalpy of Crizotinib in kJ/mol
$k_{ij}, l_{ij}, m_{ij}, n_{ij}$	Correlation parameters of Eqs. (43) to (46)
M_{CO_2}, M_s	Molar mass of CO ₂ and drug in g/mol
n_{CO_2}	Moles of CO ₂ , in mol
n_{drug}	Moles of Crizotinib drug, in mol
N	Number of experimental data for Eq. (55)

¹Department of Chemical Engineering, Faculty of Engineering, University of Kashan, Kashan 87317-53153, Iran. ²Laboratory of Supercritical Fluids and Nanotechnology, University of Kashan, Kashan 87317-53153, Iran. ³Faculty of Engineering, Modeling and Simulation Centre, University of Kashan, Kashan 87317-53153, Iran. ⁴Department of Chemical Engineering, Puducherry Technological University, Puducherry 605014, India. ✉email: sodeifian@kashanu.ac.ir

NIST	National institute of standards and technology
OF	Objective function
P_c	Critical pressure, in Pa
Q	Number of parameters in the model for Eq. (55)
P_{sub}	Pure solid sublimation pressure, in MPa
R	Universal gas constant, in J/(mol·K)
S	Solubility of Crizotinib equilibrium state, in g/L
SSE	Sum of squares error
$scCO_2$	Supercritical carbon dioxide
T	Temperature
T_c	Critical temperature
v_s	Molar volume of drug, in m^3/mol
V_1, V_s	Volume of sampling loop and collection vial, respectively, in μL
y_2, y_i	Solubility of solute mole fraction
$y_{2,i}^{exp}, y_{2,i}^{calc}$	Experimental and calculated solubility points
Z	Compressibility factor

Greek symbols

ρ	Density in kg/m^3
ρ_1	Mass density of $scCO_2$ in kg/m^3
$\hat{\phi}_2^s$	Pure substance fugacity coefficient
$\hat{\phi}_2^{scCO_2}$	Fugacity coefficient of solute in fluid phase
k	Adjustable parameters for Eqs. (6), (7)
ω	Acentric factor

Traditionally, pharmaceutical particle production processes use several organic solvents for processing their products. Quite often, remnant of solvents causes serious pollution and sometimes reactions with pharmaceutical products and result in unnecessary byproducts. These issues are effectively handled using supercritical fluid technologies (SFTs). Although, there is a scope of using several substances as supercritical fluids, CO_2 as supercritical fluid has gained importance for the last three decades. Commonly, all supercritical fluids (SCFs) have gas like diffusivities and liquid like densities makes them attractive for extraction processes. When CO_2 pressure and temperature conditions are maintained above 7.39 MPa and 304.15 K, it will act as supercritical fluid and it is commonly abbreviated as supercritical carbon dioxide ($scCO_2$)^{1–4}. Due to these features, it is used as a solvent in various process applications^{1–8}. Some of the major applications of $scCO_2$ in process industry are pharmaceutical particle size design, food processing, textile dyeing and extraction^{1–4}. Solubility information is necessary for the proper implementation of SFTs for particle size design process. The task of measuring solubility of important anti-cancer drugs in $scCO_2$ is taken in this work. In recent literature, solubilities of several anti-cancer drugs in $scCO_2$ are readily available^{8–26}, but the Crizotinib solubility in $scCO_2$ is not reported, therefore in this work for the first time its solubility is measured and reported. Crizotinib is used in the treatment of some kind of non-small cell lung cancer (NSCLC) that spreads to nearby tissues or to other parts of the body²⁷. Crizotinib helps to stop the growth of tumor cells by blocking the anaplastic lymphoma kinase (ALK) protein from working; it is also termed as fusion mutation. Appropriate dosage is attained with proper drug particle size and it is very critical for the treatment of cancer. Thus, the information obtained this study is useful in preparing various size drug particles using $scCO_2$. For practical purpose obtaining solubilities at various conditions are cumbersome hence model identification for the solubility is essential²⁸. The data developed in this work are tested with few important solubility models and three cubic equation of state models (cubic EoS) along with Kwak and Mansoori mixing rules²⁹.

The purpose of this study is in two levels. In the first level, Crizotinib solubility in $scCO_2$ is determined and in the second, data obtained are correlated with existing solubility models and with three Cubic EoS models along with Kwak and Mansoori mixing rules.

Experimental

Materials. Crizotinib is supplied by Amin Pharma company (CAS Number: 877399-52-5, mass purity > 99%). CO_2 (CAS Number: 124-38-9, mass purity > 99.9%) is purchased from Fadak company, Kashan (Iran). Dimethyl sulfoxide (DMSO, CAS Number: 67-68-5, mass purity > 99%) is procured from Sigma Aldrich company. Table 1 indicates the information about the chemicals utilized in this work.

Experiment details. The experimental setup utilized in this study is shown in Fig. 1. The details about the solubility apparatus and experimental procedure are presented in our earlier studies (Fig. 1)^{30–42}. However, a brief description is presented in this section. The method of solubility measurement utilized is classified as an isobaric-isothermal method⁴³. All measurements were made with high precision while controlling temperatures and pressures within ± 0.1 K and ± 0.1 MPa, respectively. Solubility measurements were performed at least in triplicate for each data point. For each measurement, 1 g of Crizotinib drug was used. In line with our previous works, for this compound, the observed equilibrium was within 60 min. After equilibrium, 600 μL saturated $scCO_2$ sample was collected via 2-status 6-way port valve in a DMSO preloaded vial. After discharging 600 μL

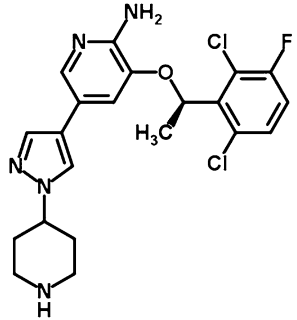
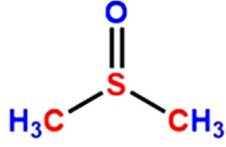
Compound	Formula	Structure	M_w (g/mol)	λ_{max} (nm)	CAS number	Minimum purity (mass) (%)
Crizotinib	$C_{21}H_{22}Cl_2FN_5O$		450.3	270	877399-52-5	99
Carbon dioxide	CO_2	$O=C=O$	44.01		124-38-9	99.99
DMSO	C_2H_6OS		78.13		67-68-5	99

Table 1. Molecular structure and physicochemical properties of used materials.

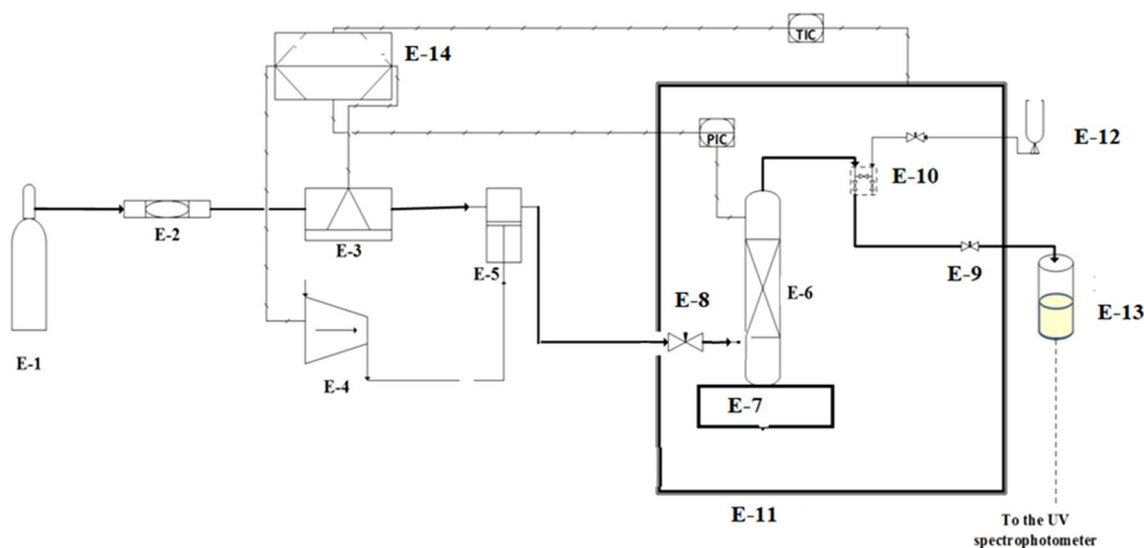


Figure 1. Experimental setup for solubility measurement, E1— CO_2 cylinder; E2—Filter; E3—Refrigerator unit; E4—Air compressor; E5—High pressure pump; E6—Equilibrium cell; E7—Magnetic stirrer; E8—Needle valve; E9—Back-pressure valve; E10 Six-port, two position valve; E11—Oven; E12—Syringe; E13—Collection vial; E14—Control panel.

saturated sc CO_2 , the port valve was washed with 1 ml DMSO. Thus, the total saturation solution was 5 ml. Drug solubility in terms of mole fraction is calculated with the following formula:

$$y_2 = \frac{n_{drug}}{n_{drug} + n_{CO_2}} \quad (1)$$

where n_{drug} is number of moles of the drug, and n_{CO_2} is number of moles of CO_2 in the sampling loop.

Furthermore, the above quantities are given as:

$$n_{drug} = \frac{C_s \cdot V_s}{M_s} \quad (2)$$

$$n_{\text{CO}_2} = \frac{V_1 \cdot \rho}{M_{\text{CO}_2}} \quad (3)$$

where C_s is the drug concentration in saturated sample vial in g/L. The volume of the sampling loop and vial collection are $V_1(\text{L}) = 600 \times 10^{-6} \text{ m}^3$ and $V_s(\text{L}) = 5 \times 10^{-3} \text{ m}^3$, respectively. The M_s and M_{CO_2} are the molecular weights of the drug and CO_2 , respectively. Solubility is also described as

$$S = \frac{C_s V_s}{V_1} \quad (4)$$

The relation between S and y_2 is

$$S = \frac{\rho M_s}{M_{\text{CO}_2}} \frac{y_2}{1 - y_2} \quad (5)$$

The Crizotinib's solubility was determined using a UV-Visible spectrophotometer (Model UNICO-4802) and DMSO solvent was used for the measurement of its solubility. Drug samples were analyzed at wave length of 270 nm.

Modeling

The Crizotinib's solubility data measured in this study is correlated by four standard solubility models namely Chrastil, Modified Chrastil, Mendez-Santiago and Teja and Bartle et al. Moreover, three cubic EoS models along with Kwak and Mansoori mixing rules are explored for the solubility data correlation. More details about the models considered in this work are presented in the following subsections⁶.

Standard solubility models. *Chrastil model*⁴⁴. Chrastil model represents by Eq. (6) that relates solubility mole fraction in terms of solvent density, association number and temperature

$$c_2 = \rho_1^\kappa \exp\left(A_1 + \frac{B_1}{T}\right) \quad (6)$$

where model constants are κ , A_1 and B_1 .

Equation (6) is alternatively represented as⁴⁵

$$y_2 = \frac{(\rho_1)^{\kappa-1} \exp\left(A_1 + \frac{B_1}{T}\right)}{\left[1 + (\rho_1)^{\kappa-1} \exp\left(A_1 + \frac{B_1}{T}\right)\right]} \quad (7)$$

where κ , A_1 and B_1 are the model parameters.

*Modified Chrastil model*⁴⁶. Dimensionally corrected Charstil model is also known as modified Charstil model and is described in terms of solvent density, association number and temperature as

$$y_2 = \left(\frac{RT\rho_1}{M_{\text{ScFf}}}\right)^{\kappa'-1} \exp\left(A_2 + \frac{B_2}{T}\right) \quad (8)$$

where κ' , A_2 and B_2 are the model parameters.

*Méndez-Santiago and Teja (MT) model*⁴⁷. Measured data self-consistency is checked with this model and represents by Eq. (9)

$$T \ln(y_2 P) = A_3 + B_3 \rho_1 + C_3 T \quad (9)$$

where A_3 and C_3 are the model parameters.

*Bartle et al., model*⁴⁸. Sublimation enthalpy of the dissolved solids in SCFs is measured with this model and stated as

$$\ln\left(\frac{y_2 P}{P_{\text{ref}}}\right) = A_4 + \frac{B_4}{T} + C_4(\rho_1 - \rho_{\text{ref}}) \quad (10)$$

where A_4 , B_4 and C_4 are the model parameters. From parameter B_4 , sublimation enthalpy is estimated ($\Delta_{\text{sub}}H = -B_4 R$).

Equation of state (EoS) modeling. There are several EoS models among them Redlich-Kwong (RK), Soave-Redlich-Kwong (SRK) and Peng-Robinson (PR) EoSs are commonly used in correlating solubility of solid compounds in scCO_2 . All these models for correlation requires adjustable interaction parameters and they are found to be temperature dependent^{49,50}. In the year 1986 Kwak and Mansoori developed a new concept in the spirit of van der Waals mixing rules (VdWmrs), which resulted in temperature independent interaction

parameters. They have demonstrated the correlating ability of RK and PR EoS²⁹. However, SRK EoS has not been explored, therefore in this work, the SRK EoS along with Kwak and Mansoori mixing rules are explored and finally two forms of solubility models for SRK EoS model is proposed. More details about the EoS modeling are presented in the following subsections.

RK EoS with Kwak and Mansoori mixing rules²⁹. RK EoS in terms of compressibility factor (Z) is given by

$$Z = \frac{v}{v-b} - \frac{a}{RT^{1.5}(v+b)} \quad (11)$$

VdWmrs for RK EoS are expressed as

$$a = \frac{\left(\sum_i^n \sum_j^n x_i x_j a_{ij}^{2/3} b_{ij}^{1/3} \right)^{3/2}}{\left(\sum_i^n \sum_j^n x_i x_j b_{ij}^{1/2} \right)^{1/2}} \quad (12)$$

$$b = \sum_i^n \sum_j^n x_i x_j b_{ij} \quad (13)$$

$$a_{ij} = (1 - k_{ij}) \sqrt{a_{ii} a_{jj}} \quad (14)$$

$$b_{ij} = (1 - l_{ij}) \frac{\left(b_{ii}^{1/3} + b_{jj}^{1/3} \right)^3}{8} \quad (15)$$

Equations (12) to (15) combined with Eq. (11), will constitute the RK EoS for mixtures, consistent with the statistical-mechanical basis of the VdW mixing rules.

PR EoS with Kwak and Mansoori mixing rules^{29,49,50}. PR EoS in terms of compressibility factor (Z) is given by

$$Z = \frac{v}{v-b} - \frac{a/RT + c - 2\sqrt{\frac{ac}{RT}}}{(v+b) + \left(\frac{b}{v}\right)(v-b)} \quad (16)$$

where

$$a(T) = 0.45724 \frac{R^2 T_c^2}{P_c} \alpha(T_r, \omega)$$

$$\alpha(T_r, \omega) = \left[1 + \left(0.37464 + 1.5422\omega - 0.26992\omega^2 \left(1 - \sqrt{T_r} \right) \right) \right]^2$$

$$b = 0.07780 \frac{RT_c}{P_c}$$

$$a = a(T_c) (1 + m)^2 \text{ and } c = a(T_c) m^2 / RT_c$$

Equation (16) provides three independent constants in terms of a , b and c . Now following the guidelines given by Kwak and Mansoori mixing rules result in the following expressions for a , b and c

$$a = \sum_i^n \sum_j^n x_i x_j a_{ij} \quad (17)$$

$$b = \sum_i^n \sum_j^n x_i x_j b_{ij} \quad (18)$$

$$c = \sum_i^n \sum_j^n x_i x_j c_{ij} \quad (19)$$

With the following interaction parameters

$$a_{ij} = (1 - k_{ij})\sqrt{a_{ii}a_{jj}} \quad (20)$$

$$b_{ij} = (1 - l_{ij}) \left(\frac{b_{ii}^{1/3} + b_{jj}^{1/3}}{2} \right)^3 \quad (21)$$

$$c_{ij} = (1 - m_{ij}) \left(\frac{c_{ii}^{1/3} + c_{jj}^{1/3}}{2} \right)^3 \quad (22)$$

Equations (17) to (22) combined with Eq. (16), will constitute the PR EoS for mixtures, consistent with the statistical-mechanical basis of the VdW mixing rules.

SRK EoS with Kwak and Mansoori mixing rules³⁸. In the following, SRK EoS is given by⁵¹

$$P = \frac{RT}{V - b} - \frac{a(T)}{V(V + b)} \quad (23)$$

where V is the molar volume and other parameters have usual meanings. The pure component parameter a , which is a function of temperature and b , which is a constant and they are obtained from the following relations.

$$a(T) = 0.42748 \frac{R^2 T_c^2}{P_c} \alpha(T) \quad (24)$$

$$b = 0.08664 \frac{RT_c}{P_c} \quad (25)$$

$$\alpha(T) = \left(1 + m \left(1 - \sqrt{\frac{T}{T_c}} \right) \right)^2 \quad (26)$$

where m is a constant given by

$$m = 0.48 + 1.574\omega - 0.176\omega^2 \quad (27)$$

where ' ω ' is the acentric factor. In 1993, Soave proposed a new $\alpha(T)$ function for heavy hydrocarbons to be used with SRK EoS⁵²

$$\alpha(T) = 1 + m \left(1 - \frac{T}{T_c} \right) + n \left(1 - \sqrt{\frac{T}{T_c}} \right)^2 \quad (28)$$

where

$$m = 0.484 + 1.515\omega - 0.044\omega^2 \quad (29)$$

$$\text{and } n = 2.756m - 0.7 \quad (30)$$

In order to separate thermodynamic variables from constants of the SRK EoS, we have adopted the following two ways.

When Eqs. (26), (27) and (23) are combined to get the following form for SRK EoS in terms of compressibility factor (Z)

$$Z = \frac{v}{v - b} - \frac{a/RT + c - 2\sqrt{\frac{ac}{RT}}}{v + b} \quad (31)$$

where

$$a = a(T_c) (1 + m)^2 \text{ and } c = a(T_c) m^2 / RT_c$$

This form of the SRK EoS suggests three independent constants namely a , b and c . Now following the guidelines given by Kwak and Mansoori mixing rules result in following expressions for a , b and c

$$a = \sum_i^n \sum_j^n x_i x_j a_{ij} \quad (32)$$

$$b = \sum_i^n \sum_j^n x_i x_j b_{ij} \quad (33)$$

$$c = \sum_i^n \sum_j^n x_i x_j c_{ij} \quad (34)$$

With the following interaction parameters:

$$a_{ij} = (1 - k_{ij}) \sqrt{a_{ii} a_{jj}} \quad (35)$$

$$b_{ij} = (1 - l_{ij}) \left(\frac{b_{ii}^{1/3} + b_{jj}^{1/3}}{2} \right)^3 \quad (36)$$

$$c_{ij} = (1 - m_{ij}) \left(\frac{c_{ii}^{1/3} + c_{jj}^{1/3}}{2} \right)^3 \quad (37)$$

Equations (32) to (37) combined with Eq. (31), will constitute the SRK EoS for mixtures, consistent with the statistical-mechanical basis of the VdW mixing rules.

When Eqs. (28), (29), (30) and (23) are combined to get the following form.

$$Z = \frac{v}{v-b} - \frac{a/RT + c - d/\sqrt{T}}{v+b} \quad (38)$$

where

$$a = a(T_c)(1 + m + n), c = \frac{a(T_c)(n - m)}{RT_c} \text{ and } d = 2n a(T_c)/R\sqrt{T_c}$$

This form of the SRK EoS suggests that four independent constants exist in the EoS namely a , b , c and d . Now following the guidelines given by Kwak and Mansoori mixing rules results in following expressions for a , b , c and d

$$a = \sum_i^n \sum_j^n x_i x_j a_{ij} \quad (39)$$

$$b = \sum_i^n \sum_j^n x_i x_j b_{ij} \quad (40)$$

$$c = \sum_i^n \sum_j^n x_i x_j c_{ij} \quad (41)$$

$$d = \sum_i^n \sum_j^n x_i x_j d_{ij} \quad (42)$$

With the following interaction parameters:

$$a_{ij} = (1 - k_{ij}) \sqrt{a_{ii} a_{jj}} \quad (43)$$

$$b_{ij} = (1 - l_{ij}) \left(\frac{b_{ii}^{1/3} + b_{jj}^{1/3}}{2} \right)^3 \quad (44)$$

$$c_{ij} = (1 - m_{ij}) \left(\frac{c_{ii}^{1/3} + c_{jj}^{1/3}}{2} \right)^3 \quad (45)$$

$$d_{ij} = (1 - n_{ij}) \left(\frac{d_{ii}^{1/3} + d_{jj}^{1/3}}{2} \right)^3 \quad (46)$$

Equations (39) to (46) combined with Eq. (38), will constitute the SRK EoS for mixtures, consistent with the statistical-mechanical basis of the VdW mixing rules.

EoS model for the solubility of solids in scCO₂. The mole fraction of dissolved solid drug *i* (solute) in Solvent scCO₂ is expressed as⁵³

$$y_i = \frac{P_i^S \hat{\phi}_i^S}{P \hat{\phi}_i^{ScCO_2}} \exp \left[\frac{(P - P_i^S) v_S}{RT} \right] \quad (47)$$

where P_i^S is the sublimation pressure and other parameters have usual meanings. The saturation fugacity coefficient ($\hat{\phi}_i^S$) is assumed to be unity. The required expression for the solid solute fugacity coefficient in the ScCO₂ ($\hat{\phi}_i^{ScCO_2}$) is calculated using three cubic EoS along with Kwak and Mansoori mixing rules. They are obtained from the following basic thermodynamic relation⁵⁴

$$\ln(\hat{\phi}_i^{ScCO_2}) = \frac{1}{RT} \int_v^\infty \left[\left(\frac{\partial P}{\partial N_i} \right)_{T,V,N_j} - \frac{RT}{v} \right] dv - \ln Z \quad (48)$$

Equations (49) to (52) represent the fugacity coefficients expressions used in this study;
For RK EoS

$$\begin{aligned} \ln(\hat{\phi}_i^{ScCO_2}) = & \ln\left(\frac{v}{v-b}\right) + \left(\frac{2\sum x_j b_{ij} - b}{v-b}\right) - \ln(Z) + \\ & \left(\frac{a(2\sum x_j b_{ij} - b)}{b^2 RT^{3/2}}\right) \left[\ln\left(\frac{v+b}{v}\right) - \frac{b}{v+b}\right] \left(3\alpha^{1/2} \left(\sum x_j a_{ij}^{2/3} b_{ij}^{1/3}\right) / b^{1/2} - \alpha^{2/3} \left(\sum x_j b_{ij} / b^{3/2}\right)\right) / b RT^{3/2} \end{aligned} \quad (49)$$

For PR EoS

$$\ln(\hat{\phi}_i^{ScF}) = \left(\frac{2\hat{B}}{b} - 1\right) (Z - 1) - \ln\left[Z\left(1 - \frac{b}{v}\right)\right] + \left[\frac{\Delta}{\sqrt{2}RTb}\right] \times \ln\left[\frac{1 + \left(1 + \sqrt{2}\right)\frac{b}{v}}{1 + \left(1 - \sqrt{2}\right)\frac{b}{v}}\right] \quad (50)$$

where

$$\begin{aligned} \Delta = & \left[\frac{E}{2} - \frac{E\hat{B}}{b} + \hat{A}\left(1 - \sqrt{RTc/a}\right) + \hat{C}\left(RT - \sqrt{RTa/c}\right)\right] \\ E = & a + cRT - 2\sqrt{acRT}; \hat{A} = \sum x_i a_{ij}; \hat{B} = \sum x_i b_{ij} \text{ and } \hat{C} = 2 \sum x_i c_{ij} \end{aligned}$$

For SRK EoS

When three parameters are considered

$$\ln(\hat{\phi}_i^{ScF}) = \frac{\hat{b}}{b} (Z - 1) - \ln\left[Z\left(1 - \frac{b}{v}\right)\right] + \left[\frac{E\hat{b}}{b^2 RT} - \frac{\hat{E}}{bRT}\right] \ln\left(1 + \frac{b}{v}\right) \quad (51)$$

where

$$\begin{aligned} E = & a + cRT - 2\sqrt{acRT} \\ \hat{E} = & \frac{1}{N} \frac{\partial(N^2 E)}{\partial N_i} = \hat{a}\left(1 - \sqrt{RTc/a}\right) + \hat{c}\left(RT - \sqrt{RTa/c}\right) \\ \hat{a} = & 2 \sum x_i a_{ij}, \hat{b} = 2 \sum x_i b_{ij} - b \text{ and } \hat{c} = 2 \sum x_i c_{ij} \end{aligned}$$

When four parameters are considered

Temperature (K) ^a	Pressure (bar) ^a	Density of ScCO ₂ (kg/m ³) ⁵⁶	y ₂ × 10 ³ (Mole fraction)	Experimental standard deviation, S(\bar{y}) × (10 ⁵)	S (Equilibrium solubility) (g/L)	Expanded uncertainty of mole fraction (10 ³ U)
308	120	769	0.483	0.005	0.038	0.025
	150	817	0.515	0.009	0.043	0.029
	180	849	0.556	0.003	0.048	0.025
	210	875	0.686	0.014	0.061	0.043
	240	896	0.730	0.015	0.067	0.042
	270	914	0.791	0.021	0.074	0.056
318	120	661	0.315	0.011	0.021	0.026
	150	744	0.566	0.015	0.043	0.039
	180	791	0.650	0.011	0.053	0.038
	210	824	0.799	0.016	0.067	0.046
	240	851	0.899	0.020	0.078	0.055
	270	872	0.958	0.041	0.085	0.090
328	120	509	0.260	0.010	0.013	0.022
	150	656	0.629	0.015	0.042	0.042
	180	725	0.749	0.012	0.056	0.043
	210	769	0.918	0.019	0.072	0.056
	240	802	0.995	0.021	0.082	0.061
	270	829	1.057	0.032	0.089	0.079
338	120	388	0.156	0.005	0.006	0.011
	150	557	0.675	0.022	0.038	0.051
	180	652	0.870	0.032	0.058	0.074
	210	710	0.993	0.035	0.072	0.088
	240	751	1.083	0.012	0.083	0.053
	270	783	1.219	0.054	0.098	0.123

Table 2. Solubility of crystalline Crizotinib in scCO₂ at various temperatures and pressures. The

experimental standard deviation was obtained by $S(y_k) = \sqrt{\frac{\sum_{j=1}^n (y_j - \bar{y})^2}{n-1}}$. Expanded uncertainty and the relative combined standard uncertainty are $(U) = k \cdot u_{combined}$ and $u_{combined}/y = \sqrt{\sum_{i=1}^N (P_i u(x_i)/x_i)^2}$ respectively. ^aStandard uncertainty u are $u(T) = \pm 0.1$ K; $u(p) = \pm 1$ bar. The value of the coverage factor $k=2$ was chosen on the basis of the level of confidence of approximately 95 percent.

$$\ln(\hat{\phi}_i^{ScF}) = \frac{\hat{b}}{b} (Z - 1) - \ln \left[Z \left(1 - \frac{b}{v} \right) \right] + \left[\frac{E\hat{b}}{b^2 RT} - \frac{\hat{E}}{bRT} \right] \ln \left(1 + \frac{b}{v} \right) \quad (52)$$

where

$$E = a + cRT - dR\sqrt{T}$$

$$\hat{E} = \frac{1}{N} \frac{\partial(N^2 E)}{\partial N_i} = \hat{a} + RT\hat{c} - R\sqrt{T}\hat{d}$$

$$\hat{a} = 2 \sum x_i a_{ij}, \quad \hat{b} = 2 \sum x_i b_{ij} - b, \quad \hat{c} = 2 \sum x_i c_{ij} \text{ and } \hat{d} = 2 \sum x_i d_{ij}$$

For the data regression, `fminsearch` (MATLAB 2019) algorithm has been used. Solubility models are regressed with the following objective function⁵⁵

$$OF = \sum_{i=1}^N \frac{|y_{2i}^{\text{exp}} - y_{2i}^{\text{calc}}|}{y_{2i}^{\text{exp}}} \quad (53)$$

Final results are indicated in terms of an average absolute relative deviation percentage (AARD %).

$$\text{AARD}(\%) = \left(100/N_i \right) \sum_{i=1}^N \frac{|y_{2i}^{\text{exp}} - y_{2i}^{\text{cal}}|}{y_{2i}^{\text{exp}}} \quad (54)$$

Serial number & name	Solubility range $\times 10^6$	T(K) and P(MPa) range	Ref.
1	Crizotinibin	308–338);(12–40)	(present work)
2	Loxoprofen	(308–338);(12–40)	9
3	Tamoxifen	(308–338);(12–40)	10
4	β -estradiol	(308–328);(10.5–22)	11,18
5	Imatinib mesylate	(308–338);(12–27)	12
6	Aprepitant	(308–338);(12–33)	13
7	Sorafenib tosylate	(308–338);(12–27)	14
8	Sunitinib malate	(308–338);(12–27)	15
9	Letrozole	(318–348);(12–36)	16
10	Azathioprine	(308–338);(12–27)	17
11	Paclitaxel	(308.15–328.15);(10–27.5)	18
12	5-fluorouracil	(308.15–328.15);(12.5–25)	11,18
13	Thymidine	(308.15–328.15);(10–30)	18
14	Busulfan	(308–328);(12–40)	19
15	Flutamide	(308–348);(12.2–35.5)	20
16	Gambogic acid	(308.15–328.15);(12.2–35.5)	21
17	Decitabine	(308–338);(12–40)	22
18	Temozolomide	(308–338);(12–40)	23
19	Tamulosin	308–338);(12–27)	24
20	Pazopanib hydrochloride	(308–338);(12–27)	25
21	Dasatinib monohydrate	(308–338);(12–27)	26

Table 3. Solubility information of the anticancer drugs.

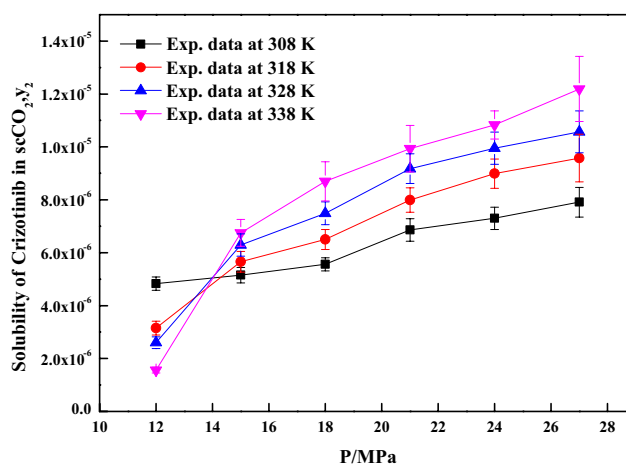


Figure 2. Solubility isotherms of Crizotinib in $scCO_2$.

Results and discussion

The reliability of the experimental setup for the solubility measurement was reported in our previous works with naphthalene and alphatocopherol compounds. Crizotinib's solubilities in $scCO_2$ at various conditions are reported in Table 2. Table 2 also indicates $scCO_2$ density obtained from NIST database⁵⁶. Table 3 indicates solubility range of some of the anticancer drugs reported in the literature. For the Crizotinib the measured solubilities are observed to range from 0.156×10^{-5} to 1.219×10^{-5} in mole fraction. Figure 2 indicates solubility isotherms and at 14.5 MPa cross over region is observed. Solubility of pure Crizotinib in $scCO_2$ the crossover point (14.5 MPa) is rather unique with respect to temperature. Below 14.5 MPa rise in temperature causes drop in solubility in $scCO_2$ phase, while above this point the opposite effect occurs. The following two ways of thermodynamic explanation may be attributed to this phenomenon as at pressures below the crossover pressure the density of the $scCO_2$ is more sensitive to temperature changes than at higher pressures. A temperature decrease in this region affects the solubility of the drug in two ways. The vapor pressure of the drug solid decrease while the density of the $scCO_2$ (proportional to its solvent power) increase thus the density effect predominates and results in the solubility increase. While on the other hand at pressures above the crossover pressure a temperature increase causes an increase the vapor pressure of the drug while the density of the $scCO_2$ decrease thus the

Model	Correlation parameters	AARD%	R ²	R ² _{adj}
Chrastil model	$\kappa = 4.0042; A_1 = -20.368; B_1 = -3677.8$	6.97	0.947	0.939
Modified Chrastil model	$\kappa' = 4.0048; A_2 = -35.727; B_2 = -2709$	6.95	0.947	0.939
Mendez-Santiago and Teja model	$A_3 = -7921.4; B_3 = 2.5303; C_3 = 9.6455$	8.27	0.93	0.919
Bartle et al., model	$A_4 = 11.249; B_4 = -5918.3; C_4 = 7.4427 \times 10^{-3}$	9.18	0.914	0.902

Table 4. Standard solubility models parameters.

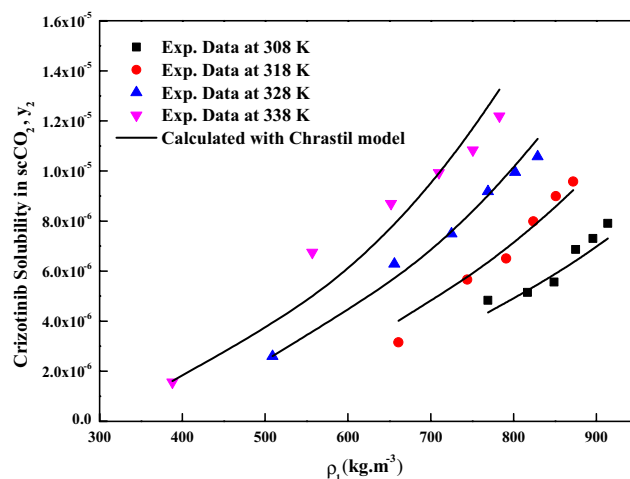


Figure 3. Crizotinib solubility in scCO_2 versus ρ_1 . Symbols are experimental data points. Solid lines are calculated solubilities with Chrastil model.

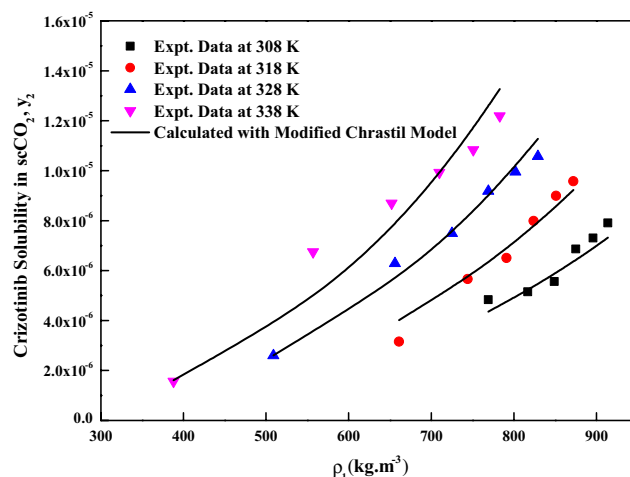


Figure 4. Crizotinib solubility in scCO_2 versus ρ_1 . Symbols are experimental data points. Solid lines are calculated solubilities with Modified Chrastil model.

vapor pressure effect predominates and the solubility increases⁵⁷. Another way to explain crossover pressure is that at crossover pressure the partial molar configurational enthalpy equals the negative of the sublimation enthalpy⁵⁸. Table 4 indicates all the standard solubility models utilized in this work. Furthermore, it also indicates all the regressed parameters along with AARD%. The correlating ability of these models are shown in Figs. 3, 4, 5 and 6. The solubility data reported in this study is considered self-consistent since all the data is aligned to a single correlation line (Fig. 5). From literature it is clear that Chrastil and modified Chrastil models are useful in calculating thermodynamic properties like heat of reaction and solvation enthalpy of the dissolution process, therefore these models are considered for the correlating the data^{31,33}. The total enthalpy of Crizotinib's dissolution in scCO_2 is calculated from the Chrastil model parameter A_1 (i.e., $\Delta H_{\text{total}} = -A_1 R$). The sublimation enthalpy of Crizotinib is calculated from Bartle model parameter (i.e., $\Delta H_{\text{sub}} = -B_4 R$). Sublimation and solvation are the

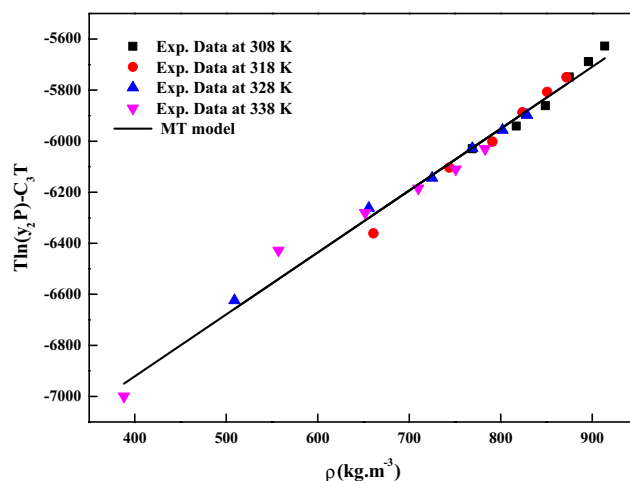


Figure 5. Self-consistency plot based on MT model.

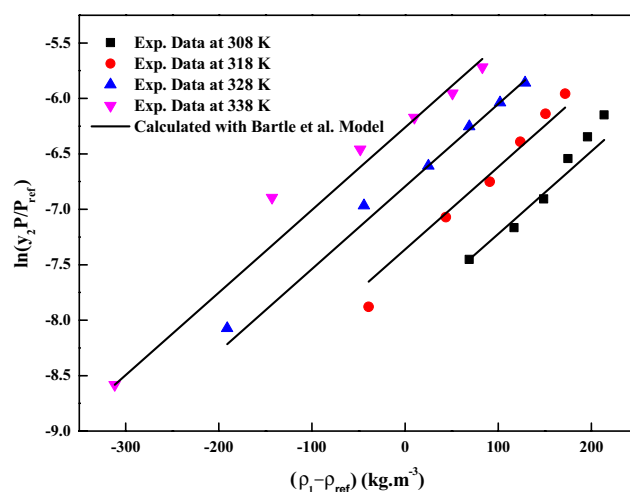


Figure 6. $\ln(y_2 P/P_{ref})$ vs. $(\rho_1 - \rho_{ref})$. Symbols are experimental data points. Solid lines are calculated solubilities with Bartle et al., model.

Model	Thermodynamic property		
	Total enthalpy, ΔH_{total} (kJ/mol)	Enthalpy of sublimation ΔH_{sub} (kJ/mol)	Enthalpy of solvation, ΔH_{sol} (kJ/mol)
Chrastil model	30.577 ^a		-18.628 ^d
Modified chrastil model	22.522 ^b		-26.683 ^c
Bartle et al., model		40.205 ^c (approximate value)	

Table 5. Calculated thermodynamic properties for Crizotinib solubility. ^dObtained as a result of difference between the ΔH_{sub} ^c and ΔH_{total} ^a. ^cObtained as a result between the ΔH_{sub} ^c and ΔH_{total} ^b.

two major steps in dissolution process and the enthalpy of solvation is calculated from the difference between $\Delta H_{total} - \Delta H_{sub}$. A negative sign is attributed to the solvation process. Similar, this approach is used to calculate all these thermodynamic quantities for modified Chrastil and Bartle models combination, thus estimated values are presented in Table 5.

The cubic EoS model requires critical properties of Crizotinib and CO₂ and these are estimated with group contribution methods based on the chemical structure^{54,59–61}. Table 6 presents all the estimated critical and physical properties of the drug considered this work. The EoS model regression results are tabulated in Table 7 along with some statistical parameters. From the AARD% it is clear that existing models (RK, SRK EoSs (three parameters) and PR EoS) are poorly correlating the solubility data (Supplementary information Fig. S1, S2, S3). The Crizotinib-scCO₂ system is highly nonlinear system and to correlate such behavior we may need more

Substance	T_c (K)	P_c (Pa)	ω	$V^s \times 10^{-6}$ (m ³ /mol)	T(K)			
					P_{sub} (Pa) ^f			
					308	318	328	338
Crizotinib	485.25 ^b	14.102 ^c	0.4394 ^d	32.12 ^e	1072	1628	2398	3433
CO ₂	304.18	73.8	0.225					

Table 6. Critical and physical properties of Crizotinib and CO₂. ^a T_c : critical temperature; P_c : critical pressure; ω : acentric factor; V^s : solid molar volume; T: Temperature. ^bEstimated by Fedors method. ^cEstimated by Joback and Reed method. ^dEstimated by Lee-Kesler vapour pressure relations (Note: the required normal boiling temperature (at 1.0 atm), T_b is estimated with Klincewicz relation, $T_c = 50.2 - 0.16 M + 1.41 T_b$, where M is molecular weight). ^eEstimated by Immirzi, A., Perini, B method. ^fEstimated by Lee-Kesler vapour method.

Model	Correlation parameters	AARD%	R ²	R ² _{adj}
RK EoS + Kwak and Mansoori mixing rules	$k_{ij} = -0.137$	21.7	0.44	0.388
	$l_{ij} = -0.1476$			
PR EoS + Kwak and Mansoori mixing rules	$k_{ij} = -0.775$	16.2	0.888	0.871
	$l_{ij} = -0.297$			
	$m_{ij} = 1.810$			
SRK EoS + Kwak and Mansoori mixing rules (three parameters)	$k_{ij} = 0.367$	22.8	0.797	0.767
	$l_{ij} = -0.179$			
SRK EoS + Kwak and Mansoori mixing rules (four parameters)	$k_{ij} = 0.256$	8.07	0.921	0.906
	$l_{ij} = -0.236$			
	$m_{ij} = -0.293$			
	$n_{ij} = 0.436$			

Table 7. Calculated results for the Cubic EoS + Kwak and Mansoori mixing rules.

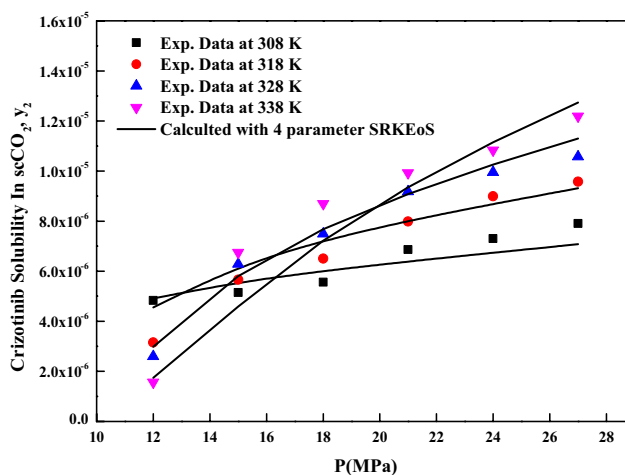


Figure 7. Crizotinib solubility in scCO₂ vs. P. Symbols are experimental data points. Solid lines are calculated solubilities with SRK EoS + Kwak and Mansoori mixing rules (four parameters model).

adjustable parameter, therefore a new form of solubility model based on Kwak and Mansoori guidelines for SRK EoS is proposed. In the new model, one extra parameter is introduced in the term 'a' when compared to existing three parameter SRK EoS. Since more parameters are present in the model the regression results will be better in terms of AARD%. Thus, the proposed SRK EoS model is having four parameters. Further the new EoS model is found to correlate the data better than the existing EoS models. From the AARD% it is clear that four parameter SRK EoS correlates the solubility data much better than PR EoS model. Experimental data points and four parameter SRK EoS model predictions are depicted in Fig. 7. Due to poor correlation the RK, PR and three parameter SRK EoSs results are not shown as figures. Overall, four parameter SRK EoS is able to provide satisfactory solubility correlation results. The success of four parameter SRK EoS may be attributed to its number of parameters that constitute the model.

Model	SSE($\cdot 10^{11}$)	RMSE($\cdot 10^7$)	N	Q	AIC	AIC _c
Standard Solubility Models						
Chrastil model	1.034	6.564	3	24	-677.4	-676.2
Modified Chrastil model	1.033	6.559	3	24	-677.4	-676.2
Mendez-Teja model	1.384	7.59	3	24	-670.4	-669.2
Bartle et al., model	1.739	8.51	5	24	-664.9	-663.7
Cubic EoS models						
RK EoS model + Kwak and Mansoori mixing rules	11.90	22.267	2	24	-620.7	-620.1
PR EoS model + Kwak and Mansoori mixing rules	3.354	11.822	3	24	-649.1	-647.9
SRK EoS model + Kwak and Mansoori mixing rules(Three parameters model)	3.576	12.207	3	24	-647.6	-646.4
SRK EoS model + Kwak and Mansoori mixing rules(four parameters model)	1.324	7.428	4	24	-669.2	-667.3

Table 8. Models and their statistical parameters.

Goodness of the models is quantified using an indicator known as Akaike Information Criterion (AIC) and corrected AIC (AIC_c)^{62–64}. As we know, if the experimental data points are less than forty, the AIC_c is employed. An expression that relates AIC_c with AIC, number of data points (N) and number of parameters in the model (Q), is

$$AIC_c = AIC + \frac{2Q(Q+1)}{N-Q-1} \quad (55)$$

where AIC is $N \ln(SSE/N) + 2Q$ and SSE is error sum of squares. According to this indicator, the best model would have least AIC_c value. The summary of AIC, AIC_c, SSE and RMSD values for various models are presented in Table 8. From AIC_c values, it is clear that Chrastil and modified Chrastil models are the better models, whereas four parameter SRK EoS model is the best model among EoS models.

Conclusions

Solubilities of Crizotinib in ScCO₂ at various conditions are presented at (T = 308, 318, 328 and 338 K) and (P = 12, 15, 18, 21, 24 and 27 MPa), for the first time. The measured solubilities are in the range from 0.156×10^{-5} to 1.219×10^{-5} in terms of mole fraction. The obtained data was modeled with four standard models and three EoS models combining with Kwak and Mansoori mixing rules. Chrastil and Modified Chrastil models are observed to correlate the data with least AARD% and AIC_c values. Among EoS models, four parameter SRK EoS model is able to correlate the data satisfactorily and on par with standard models. Finally, all the standard solubility models considered in this study are able to provide reasonable solubility results.

Data availability

The datasets generated and/or analyzed during the current study are not publicly available due to confidential cases and are available from the corresponding author on reasonable request.

Received: 19 August 2022; Accepted: 13 October 2022

Published online: 19 October 2022

References

- Subramaniam, B., Rajewski, R. A. & Snavely, K. Pharmaceutical processing with supercritical carbon dioxide. *J. Pharm. Sci.* **86**(8), 885–890 (1997).
- Elvassore, NKI. Pharmaceutical processing with supercritical fluids. In Bertucco, AGVG, (Ed) *High Pressure Process Technology: Fundamentals and Applications*. pp. 612–625. (Elsevier Science, Springer, 2001)
- Gupta, R. B., Chattopadhyay, P. Method of forming nanoparticles and microparticles of controllable size using supercritical fluids and ultrasound. *US patent No. 20020000681* (2002).
- Reverchon, E., Adami, R., Caputo, G. & De Marco, I. Spherical microparticles production by supercritical antisolvent precipitation: Interpretation of results. *J. Supercrit. Fluids* **47**(1), 70–84 (2008).
- Sodeifian, G., Ardestani, N. S., Sajadian, S. A. & Panah, H. S. Experimental measurements and thermodynamic modeling of Coumarin-7 solid solubility in supercritical carbon dioxide: Production of nanoparticles via RESS method. *Fluid Phase Equilib.* **483**, 122–143 (2019).
- Sodeifian, G., Alwi, R. S., Razmimanesh, F. & Roshanghias, A. Solubility of pazopanib hydrochloride (PZH, anticancer drug) in supercritical CO₂: Experimental and thermodynamic modeling. *J. Supercrit. Fluids* **190**, 105759 (2022).
- Sodeifian, G., Sajadian, S. A., Ardestani, N. S. & Razmimanesh, F. Production of loratadine drug nanoparticles using ultrasonic-assisted rapid expansion of supercritical solution into aqueous solution (US-RESSAS). *J. Supercrit. Fluids* **147**, 241–253 (2019).
- Alwi, R. S. & Garlapati, C. New correlations for the solubility of anticancer drugs in supercritical carbon dioxide. *Chem. Pap.* **76**, 1385–1399 (2022).
- Zabihi, S. *et al.* Loxoprofen solubility in supercritical carbon dioxide: Experimental and modeling approaches. *J. Chem. Eng. Data* **65**, 4613–4620 (2020).
- Pishnamazi, M. *et al.* Thermodynamic modelling and experimental validation of pharmaceutical solubility in supercritical solvent. *J. Mol. Liq.* **319**, 114120 (2020).
- Guney, O. & Akgerman, A. Solubilities of 5Fluorouracil and β -estradiol in supercritical carbon dioxide. *J. Chem. Eng. Data* **45**(6), 1049–1052 (2000).

12. Sodeifian, G., Razmimanesh, F. & Sajadian, S. A. Solubility measurement of a chemotherapeutic agent (Imatinib mesylate) in supercritical carbon dioxide: Assessment of new empirical model. *J. Supercrit. Fluids* **146**, 89–99 (2019).
13. Sodeifian, G., Sajadian, S. A. & Ardestani, N. S. Determination of solubility of aprepitant (an antiemetic drug for chemotherapy) in supercritical carbon dioxide: Empirical and thermodynamic models. *J. Supercrit. Fluids* **128**, 102–111 (2017).
14. Sodeifian, G., Razmimanesh, F., Sajadian, S. A. & Hazaveie, S. M. Experimental data and thermodynamic modeling of solubility of sorafenib tosylate, as an anti-cancer drug, in supercritical carbon dioxide: Evaluation of Wong-Sandler mixing rule. *J. Chem. Thermodyn.* **142**, 105998 (2020).
15. Sodeifian, G., Razmimanesh, F. & Sajadian, S. A. Prediction of solubility of sunitinib malate (an anti-cancer drug) in supercritical carbon dioxide (SC-CO₂): Experimental correlations and thermodynamic modeling. *J. Mol. Liq.* **297**, 111740 (2020).
16. Sodeifian, G. & Sajadian, S. A. Solubility measurement and preparation of nanoparticles of an anticancer drug (Letrozole) using rapid expansion of supercritical solutions with solid cosolvent (RESS-SC). *J. Supercrit. Fluids* **133**(1), 239–252 (2018).
17. Sodeifian, G., Razmimanesh, F., Ardestani, N. S. & Sajadian, S. A. Experimental data and thermodynamic modeling of solubility of Azathioprine, as an immunosuppressive and anti-cancer drug, in supercritical carbon dioxide. *J. Mol. Liq.* **299**, 112179 (2019).
18. Suleiman, D., Antonio Estévez, L., Pulido, J. C., García, J. E. & Mojica, C. Solubility of anti-inflammatory, anti-cancer, and anti-HIV drugs in supercritical carbon dioxide. *J. Chem. Eng. Data* **50**, 1234–1241 (2005).
19. Pishnamazi, M. *et al.* Measuring solubility of a chemotherapy-anti cancer drug (busulfan) in supercritical carbon dioxide. *J. Mol. Liq.* **317**, 113954 (2020).
20. Yamini, Y. *et al.* Solubilities of flutamide, dutasteride, and finasteride as antiandrogenic agents, in supercritical carbon dioxide: Measurement and correlation. *J. Chem. Eng. Data* **55**(2), 1056–1059 (2010).
21. Xiang, S. T., Chen, B. Q., Kankala, R. K., Wang, S. B. & Chen, A. Z. Solubility measurement and RESOLV-assisted nonionization of gambogic acid in supercritical carbon dioxide for cancer therapy. *J. Supercrit. Fluids* **150**, 147–155 (2019).
22. Pishnamazi, M. *et al.* Experimental and thermodynamic modeling decitabine anti cancer drug solubility in supercritical carbon dioxide. *Sci. Rep.* **11**, 1075 (2021).
23. Zabihi, S. *et al.* Thermodynamic study on solubility of brain tumor drug in supercritical solvent: Temozolomide case study. *J. Mol. Liq.* **321**, 114926 (2021).
24. Hazaveie, S. M., Sodeifian, G. & Sajadian, S. A. Measurement and thermodynamic modeling of solubility of tamsulosin drug (anti cancer and anti-prostatic tumor activity) in supercritical carbon dioxide. *J. Supercrit. Fluids* **163**, 104875 (2020).
25. Sodeifian, G., Alwi, R. S., Razmimanesh, F. & Roshanghias, A. Solubility of pazopanib hydrochloride (PZH, anticancer drug) in supercritical CO₂: Experimental and thermodynamic modeling. *J. Supercrit. Fluids* **190**, 105759 (2022).
26. Sodeifian, G., Alwi, R. S., Razmimanesh, F. & Abadian, M. Solubility of dasatinib monohydrate anticancer drug in supercritical CO₂: Experimental and thermodynamic modeling. *J. Mol. Liq.* **346**, 117899 (2022).
27. Frampton, J. E. Crizotinib: A review of its use in the treatment of anaplastic lymphoma kinase-positive, advanced non-small cell lung cancer. *Drugs* **73**(18), 2031–2051 (2013).
28. Mahesh, G. & Garlapati, C. Modelling of solubility of some parabens in supercritical carbon dioxide and new correlations. *Arab. J. Sci. Eng.* **47**, 5533–5545 (2021).
29. Kwak, T. & Mansoori, G. Van der Waals mixing rules for cubic equations of state. Applications for supercritical fluid extraction modelling. *Chem. Eng. Sci.* **41**(5), 1303–1309 (1986).
30. Sodeifian, G., Alwi, R. S., Razmimanesh, F. & Tamura, K. Solubility of quetiapine hemifumarate (antipsychotic drug) in supercritical carbon dioxide: Experimental, modeling and hansen solubility parameter application. *Fluid Phase Equilib.* **537**, 113003 (2021).
31. Sodeifian, G., Garlapati, C., Razmimanesh, F. & Ghanaat-Ghamsari, M. Measurement and modeling of clemastine fumarate (antihistamine drug) solubility in supercritical carbon dioxide. *Sci. Rep.* **11**(1), 1–16 (2021).
32. Sodeifian, G., Nasri, L., Razmimanesh, F. & Abadian, M. CO₂ Utilization for determining solubility of teriflunomide (immunomodulatory agent) in supercritical carbon dioxide. Experimental investigation and thermodynamic modeling. *J. Util.* **58**, 101931 (2022).
33. Sodeifian, G., Ardestani, N. S., Sajadian, S. A. & Panah, H. S. Measurement, correlation and thermodynamic modeling of the solubility of Ketotifen fumarate (KTF) in supercritical carbon dioxide: Evaluation of PCP-SAFT equation of state. *J. Fluid Phase Equilib.* **458**, 102–114 (2018).
34. Sodeifian, G., Detakhsheshpour, R. & Sajadian, S. A. Experimental study and thermodynamic modeling of Esomeprazole (proton-pump inhibitor drug for stomach acid reduction) solubility in supercritical carbon dioxide. *J. Supercrit. Fluids* **154**, 104606 (2019).
35. Sodeifian, G., Garlapati, C., Razmimanesh, F. & Sodeifian, F. Solubility of amlodipine besylate (calcium channel blocker drug) in supercritical carbon dioxide: Measurement and correlations. *J. Chem. Eng. Data* **66**(2), 1119–1131 (2021).
36. Sodeifian, G., Garlapati, C., Razmimanesh, F. & Sodeifian, F. The solubility of sulfabenzamide (an antibacterial drug) in supercritical carbon dioxide: Evaluation of a new thermodynamic model. *J. Mol. Liq.* **335**, 116446 (2021).
37. Sodeifian, G., Hazaveie, S. M., Sajadian, S. A. & Saadati Ardestani, N. Determination of the solubility of the repaglinide drug in supercritical carbon dioxide: Experimental data and thermodynamic modeling. *J. Chem. Eng. Data* **64**(12), 5338–5348 (2019).
38. Sodeifian, G., Hsieh, C.-M., Derakhsheshpour, R., Chen, Y.-M. & Razmimanesh, F. Measurement and modeling of metoclopramide hydrochloride (anti-emetic drug) solubility in supercritical carbon dioxide. *Arab. J. Chem.* **15**, 103876 (2022).
39. Sodeifian, G., Nasri, L., Razmimanesh, F. & Abadian, M. Measuring and modeling the solubility of an antihypertensive drug (losartan potassium, Cozaar) in supercritical carbon dioxide. *J. Mol. Liq.* **331**, 115745 (2021).
40. Sodeifian, G., Razmimanesh, F., Sajadian, S. A. & Panah, H. S. Solubility measurement of an antihistamine drug (Loratadine) in supercritical carbon dioxide: Assessment of qCPA and PCP-SAFT equations of state. *J. Fluid Phase Equilib.* **472**, 147–159 (2018).
41. Sodeifian, G., Sajadian, S. A. & Razmimanesh, F. Solubility of an antiarrhythmic drug (amiodarone hydrochloride) in supercritical carbon dioxide: Experimental and modeling. *Fluid Phase Equilib.* **450**, 149–159 (2017).
42. Sodeifian, G., Sajadian, S. A., Razmimanesh, F. & Hazaveie, S. M. Solubility of Ketoconazole (antifungal drug) in SC-CO₂ for binary and ternary systems: Measurements and empirical correlations. *Sci. Rep.* **11**(1), 1–13 (2021).
43. Peper, S., Fonseca, J. M. & Dohrn, R. High-pressure fluid-phase equilibria: Trends, recent developments, and systems investigated (2009–2012). *Fluid Phase Equilib.* **484**, 126–224 (2019).
44. Chrastil, J. Solubility of solids and liquids in supercritical gases. *J. Phys. Chem.* **86**(15), 3016–3021 (1982).
45. Sridar, R., Bhowal, A. & Garlapati, C. A new model for the solubility of dye compounds in supercritical carbon dioxide. *Thermochim. Acta* **561**, 91–97 (2013).
46. Garlapati, C. & Madras, G. Solubilities of palmitic and stearic fatty acids in supercritical carbon dioxide. *J. Chem. Thermodyn.* **42**(2), 193–197 (2010).
47. Méndez-Santiago, J. & Teja, A. S. The solubility of solids in supercritical fluids. *Fluid Phase Equilib.* **158**, 501–510 (1999).
48. Bartle, K. D., Clifford, A., Jafar, S. & Shilstone, G. Solubilities of solids and liquids of low volatility in supercritical carbon dioxide. *J. Phys. Chem. Ref. Data* **20**(4), 713–756 (1991).
49. Garlapati, C. & Madras, G. Temperature independent mixing rules to correlate the solubilities of antibiotics and anti-inflammatory drugs in SCCO₂. *Thermochim. Acta* **496**(1–2), 54–58 (2009).
50. Valderrama, J. O. & Alvarez, V. H. Temperature independent mixing rules to correlate the solubility of solids in supercritical carbon dioxide. *J. Supercrit. Fluids* **32**(1–3), 37–46 (2004).
51. Soave, G. Equilibrium constants from a modified Redlich-Kwong equation of state. *Chem. Eng. Sci.* **27**, 1197–1203 (1972).
52. Soave, G. Improving the treatment of heavy hydrocarbons by the SRK EOS. *Fluid Phase Equilib.* **84**, 339–342 (1993).

53. Alwi, R. S. & Garlapati, C. A new semi empirical model for the solubility of dyestuffs in supercritical carbon dioxide. *Chem. Pap.* **75**(6), 2585–2595 (2021).
54. Reid, R. C., Prausnitz, J. M., Poling, B. E. The properties of gases and liquids. (1987).
55. Valderrama, J. O. & Alvarez, V. H. Correct way of representing results when modelling supercritical phase equilibria using equation of state. *Can. J. Chem. Eng.* **83**(3), 578–581 (2008).
56. <https://webbook.nist.gov/chemistry/01> In Institute of Standards and Technology U.S. Department of Commerce (2018).
57. Chimowitz, E. H. & Pennisi, K. J. Process synthesis concepts for supercritical gas extraction in the crossover region. *AIChE J.* **32**(10), 1665–1676 (1986).
58. Johnston, K. P., Barry, S. E., Read, N. K. & Holcomb, T. R. Separation of isomers using retrograde crystallization from supercritical fluids. *Ind. Eng. Chem. Res.* **26**, 2372–2377 (1987).
59. Fedors, R. F. A method for estimating both the solubility parameters and molar volumes of liquids. *Polym. Eng. Sci.* **14**(2), 147–154 (1974).
60. Immirzi, A. & Perini, B. Prediction of density in organic crystals. *Acta Crystallographica Sect. A Crystal Phys. Diffr. Theor. Gen. Crystallogr.* **33**(1), 216–218 (1977).
61. Lyman, W. J., Reehl, W.F. & Rosenblatt, D. H. In *Hand book of chemical property estimation methods*. (McGraw-Hill, 1982)
62. Akaike, H. Information theory and an extension of the maximum likelihood principle. In Petrov, B. N. C. F. (Ed.) *Proceedings of the second international symposium on information theory*. pp 267–81. (Akademiai Kiado, Budapest, 1973)
63. Burnham, K. P. & Anderson, D. R. Multimodel inference: Understanding AIC and BIC in model selection. *Sociol. Methods Res.* **33**(2), 261–304 (2004).
64. Kletting, P. & Glatting, G. Model selection for time-activity curves: The corrected Akaike information criterion and the F-test. *Z. Med. Phys.* **19**(3), 200–206 (2009).

Acknowledgements

Authors wish to acknowledge the research deputy of University of Kashan (Grant # Pajoohaneh-1401/28) for the financial support of this valuable project.

Author contributions

G.S.: Conceptualization, Methodology, Validation, Investigation, Supervision, Project administration, Writing-review & editing; C.G.: Methodology, Investigation, Software, Writing-original draft; A.R.: Resources. All authors reviewed the manuscript.

Competing interests

The authors declare no competing interests.

Additional information

Supplementary Information The online version contains supplementary material available at <https://doi.org/10.1038/s41598-022-22366-y>.

Correspondence and requests for materials should be addressed to G.S.

Reprints and permissions information is available at www.nature.com/reprints.

Publisher's note Springer Nature remains neutral with regard to jurisdictional claims in published maps and institutional affiliations.



Open Access This article is licensed under a Creative Commons Attribution 4.0 International License, which permits use, sharing, adaptation, distribution and reproduction in any medium or format, as long as you give appropriate credit to the original author(s) and the source, provide a link to the Creative Commons licence, and indicate if changes were made. The images or other third party material in this article are included in the article's Creative Commons licence, unless indicated otherwise in a credit line to the material. If material is not included in the article's Creative Commons licence and your intended use is not permitted by statutory regulation or exceeds the permitted use, you will need to obtain permission directly from the copyright holder. To view a copy of this licence, visit <http://creativecommons.org/licenses/by/4.0/>.

© The Author(s) 2022